PCCP

COMMUNICATION

Cite this: *Phys. Chem. Chem. Phys.*, 2021, **23**, 24541

Received 30th August 2021,
Accepted 19th October 2021

DOI: 10.1039/d1cp03972e

rsc.li/pccp

Conservation of the Stokes–Einstein relation in supercooled water†

Gan Ren[a] and Yanting Wang*[bc]

The Stokes–Einstein (SE) relation is commonly regarded as being breakdown in supercooled water. However, this conclusion is drawn by testing the validity of some variants of the SE relation rather than its original form, and it appears conflicting with the fact that supercooled water is in its local equilibrium. In this work, we show by molecular dynamics simulations that the Stokes–Einstein relation is indeed conserved in supercooled water. The inconsistency between the original SE relation and its variants comes from two facts: (1) the substitutes of the shear viscosity in the SE variants are only approximate relations; and (2) the effective hydrodynamic radius actually decreases with decreasing temperature, instead of being a constant as assumed in the SE variants.

The Stokes–Einstein (SE) relation[1] combines the Einstein relation $D = k_BT/\alpha$ and Stokes' formula for hard-sphere particles moving in a viscous fluid $\alpha = C\eta a$, where D is the diffusion coefficient, k_B is the Boltzmann constant, T is the temperature, α is the frictional coefficient, η is the shear viscosity, a is the effective hydrodynamic radius, and C is a constant depending on the boundary conditions. The SE relation has been successfully applied to many cases, such as colloids,[2,3] solutions,[4] hard sphere systems,[5] and pure liquids.[6] On the other hand, it is also frequently found to break down in complex and supercooled liquids, especially in supercooled water.[7–11] However, instead of its original form, the validity of the SE relation in supercooled water was tested by its three variants, $D \sim T/\eta$,[9,10] $D \sim \tau^{-1}$,[12,13] and $D \sim T/\tau$,[7,14] where τ is the structural relaxation time. The expression $D \sim T/\eta$ becomes a substitute by assuming that a is a constant in homogeneous liquids. Due to the difficulty of accurately determining η in molecular dynamics (MD) simulations (although it can be done to a certain extent by non-equilibrium MD simulations as we do in this work), τ is frequently adopted to replace η, resulting in the variant $D \sim \tau^{-1}$ under a further assumption that τ has a similar temperature dependence as η/T.[12,13] Finally, besides the assumption that a is a constant, the variant $D \sim T/\tau$ comes from the approximate relation $\eta = G_\infty\tau$,[7,14] where G_∞ is the instantaneous shear modulus presumed to be a constant.

Because the above assumptions are *ad hoc*, testing the validity of the SE relation by its variants in supercooled water is questionable. Furthermore, since supercooled water is still in its local equilibrium, it is not unreasonable that the SE relation is actually conserved. In this work, we perform MD simulations with the TIP5P water model and the Jagla fluid model, respectively, to check the consistency between the original SE relation and its variants in supercooled water. These two models were adopted because they had previously been used to explore the anomaly and the validity of the SE relation in supercooled water.[7,14–16] Below the simulation results with the TIP5P model are presented in the main text, and those with the Jagla model can be found in the ESI.† The simulation results with both models qualitatively agree with each other very well.

All our MD simulations were performed with the GROMACS simulation package.[17,18] The periodic boundary conditions were applied in all three directions of the Cartesian space and the system temperature was kept constant using a Nosé–Hoover thermostat with a time constant of 0.2 ps.[19,20] The particle mesh Ewald algorithm[21] was employed to calculate the long-range electrostatic interactions with a cutoff of 1.2 nm in the real space and the van der Waals interactions were calculated directly with a truncated spherical cutoff of 1.2 nm. The system simulated with the TIP5P model consists of 2048 water molecules with a constant density of $\rho = 0.976$ g cm^{-3}. Twenty-five simulated temperatures are distributed in the range of 240–390 K. The simulation time step is 1 fs and the simulated

---

[a] *School of Science, Civil Aviation Flight University of China, Guanghan 628307, China*

[b] *CAS Key Laboratory of Theoretical Physics, Institute of Theoretical Physics, Chinese Academy of Sciences, Beijing 100190, China. E-mail: wangyt@itp.ac.cn*

[c] *School of Physical Sciences, University of Chinese Academy of Sciences, Beijing 100049, China*

† Electronic supplementary information (ESI) available: Simulation details for the Jagla fluid model; diffusion constant, structural relaxation time, viscosity and frictional coefficient for TIP5P and Jagla at different temperatures; Stokes–Einstein relation and its variants for the Jagla fluid model. See DOI: 10.1039/d1cp03972e

time for each case ranges from 1 to 100 ns depending on the temperature.

To examine the three variants, we have to first determine the diffusion coefficient D, structural relaxation time τ, shear viscosity η, and frictional coefficient α. The diffusion coefficient is calculated *via* its asymptotic relation with the mean square displacement $D = \lim_{t\to\infty} \langle \Delta \mathbf{r}^2(t) \rangle / 6t$, where $\Delta\mathbf{r}(t)$ is the particle position displacement and $\langle\rangle$ denotes the ensemble average. The calculated D values are plotted in Fig. S1a (ESI†).

The structural relaxation of water is described by the self-intermediate scattering function $F_s(k,t) = \frac{1}{N}\sum_i^N \langle e^{ik\cdot\Delta\mathbf{r}(t)} \rangle$, where N is the number of water molecules, the wavevector k is usually chosen as where the first maximum of the static structure factor is allocated, which is 24.5 nm^{-1} for the TIP5P model. Since the structural relaxation usually follows an exponential relaxation, τ is determined by $F_s(k,\tau) = e^{-1}$. The calculated τ values as a function of T with k values within the range of 2.5–24.5 nm^{-1} with an interval of 2 nm^{-1} are plotted in Fig. S2a (ESI†).

The method proposed by Hess[22] was employed to determine the shear viscosity because of its reliability and fast convergence. In this method, an external force $a_x = A\cos(qz)$ is applied in the X direction, where A is the maximum of a_x and $q = 2\pi/l$ with l being the simulation box size and z being the position in the Z direction. The steady-state solution of the Navier–Stokes equation $\partial_t u_x + u_x\cdot\nabla u_x = -(\eta/\rho)\nabla^2 u_x + a_x$ in the X direction is $u_x(z) = V\cos(qz)$, where V is the maximum value of $u_x(z)$. Therefore, the shear viscosity can be calculated by $\eta = A\rho/Vq^2$. Because both ρ and q are constants, we use the ratio A/V to evaluate η, whose values are plotted in Fig. S3a (ESI†).

The frictional coefficient α was determined by applying a constant external force F_e on 128 selected molecules and all other particles are treated as the background media. In the linear-response regime, the frictional force on an ion $f_r = \alpha v_r$ is equal to F_e after reaching the non-equilibrium steady state, where $v_r = \lim_{t\to\infty} \langle r(t) \rangle / t$. The frictional coefficient can thus be determined by $\alpha = F_e/v_r$, as plotted in Fig. S4a (ESI†).

Based on D, τ, η, and α shown in Fig. S1–S4 (ESI†), we fit our simulation data with the three formulas $D \sim \tau^{-\xi_1}$, $D \sim (\tau/T)^{-\xi_2}$ (τ calculated with k = 24.5 nm^{-1}), and $D \sim (\eta/T)^{-\xi_3}$ to test the three variants. Moreover, $D \sim (\alpha/T)^{-\xi_4}$ are fitted to test the Einstein relation. A variant or the Einstein relation is valid if the corresponding exponent $\xi_i \simeq 1.0$ (i = 1, 2, 3 or 4), and invalid otherwise. To facilitate the determination of the exponents, the logarithm of D *versus* logarithms of τ, τ/T, η/T, and α/T, respectively, are calculated and plotted in Fig. 1.

It can be seen from Fig. 1a and b that both ξ_1 and ξ_2 deviate significantly from 1.0, indicating the breakdown of $D \sim \tau^{-1}$ and $D \sim T/\tau$. Each set of the data can be divided into two parts by a crossover temperature T_x, and each part can be well fitted by a fractional form with a different ξ value. The T_x value is 285 K for $D \sim \tau^{-\xi_1}$ and 280 K for $D \sim (\tau/T)^{-\xi_2}$, both with ξ_1, $\xi_2 < 1$ at $T > T_x$ and ξ_1, $\xi_2 > 1$ at $T > T_x$. Similar phenomena have been observed by Chen *et al.*[11,13] and Xu *et al.*[7] As shown in Fig. 1c, $D \sim (\eta/T)^{-\xi_3}$ also follows two fractional forms with $T_x \approx 280$ K. While $\xi_3 = 0.99$ manifests that $D \sim T/\eta$ is valid at $T > T_x$, $\xi_3 = 0.82$ suggests its breakdown at $T > T_x$. This agrees with not only the experimental observation in water that $\xi_3 = 1$ at high temperatures and $\xi_3 = 0.8$ at low temperatures,[10] but also the simulation results with the TIP4P/2005 water model.[9] By contrast, as shown in Fig. 1d, the fitted exponent $\xi = 1.01$ for the whole simulated temperature range is so close to 1.0 that it strongly supports the conservation of the Einstein relation $D = k_BT/\alpha$, naturally consistent with the fact that supercooled water, although metastable, is still in its local equilibrium.

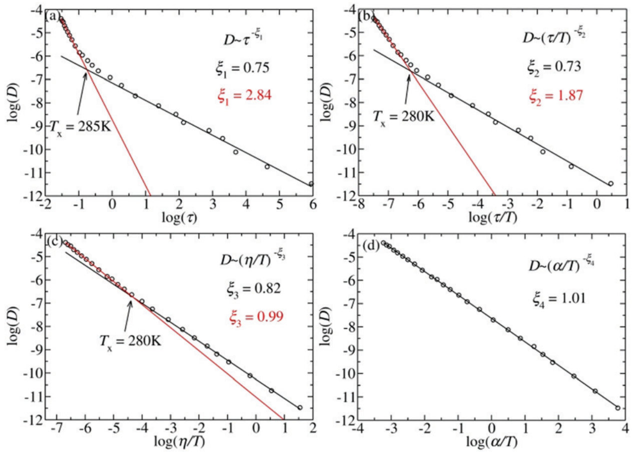

Fig. 1 Verification of the validity of the three variants $D \sim \tau^{-1}$ (a), $D \sim T/\tau$ (b), and $D \sim T/\eta$ (c), and the Einstein relation $D \sim T/\alpha$ (d). The calculated data are represented by circles and fitted by $D \sim \tau^{-\xi_1}$, $D \sim (\tau/T)^{-\xi_2}$, $D \sim (\eta/T)^{-\xi_3}$, and $D \sim (\alpha/T)^{-\xi_4}$, respectively. The fitted exponent ξ is written in the same colour as the corresponding solid fitting line.

Fig. 2a and b show the k dependence of $D \sim \tau^{-\xi_1}$ and $D \sim (\tau/T)^{-\xi_2}$, which can be understood as follows. The variant $D \sim \tau^{-1}$ can be exact only if particle displacement follows Gaussian, but it does not even in a system as simple as a hard

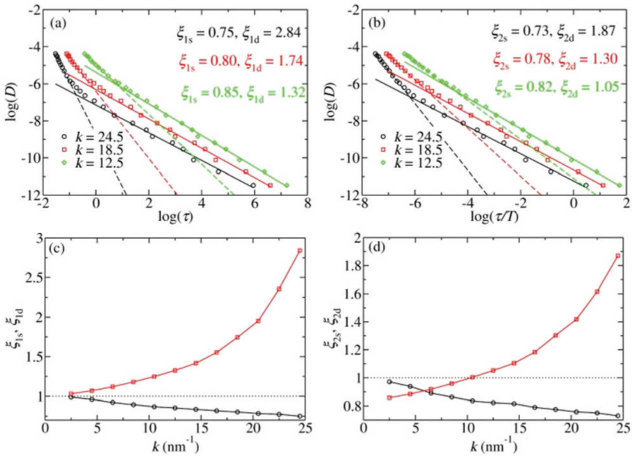

Fig. 2 Fitting of the k-dependent exponents ξ_1 by $D \sim \tau^{-\xi_1}$ (a) and ξ_2 by $D \sim (\tau/T)^{-\xi_2}$ (b), as well as ξ_1 *vs.* k (c) and ξ_2 *vs.* k (d). In (a and b), the calculated data are represented by different symbols and the fitted exponent is written in the same color as the corresponding fitting line. In (c and d), black circles represent ξ_{1s}, ξ_{2s} and red squares are ξ_{1d}, ξ_{2d}.

sphere system because of the long-time tail effect,[23] resulting in the self-intermediate scattering function described by[24]

$$\ln F_s(k,t) = -Dk^2t + 3(2\gamma/\pi)^{1/2}Dk^2(t\tau_c)^{1/2} + \cdots \qquad (1)$$

where $\gamma = 1$ for a pure liquid, $\tau_c = m/\alpha$ is the characteristic time for the Brownian motion, and m is the particle mass. The first term at the right hand side corresponds to the Gaussian case, and the second term corresponds to the memory effect. The contribution of the second term to τ is usually smaller than the first one, but it does alter τ from Gaussian and can be omitted only in the long-wavelength limit $k \to 0$.

The data in Fig. 2a and b can also be well fitted by two fractional forms with a crossover temperature, and the corresponding exponents with respect to more k values are shown in Fig. 2c and d. Fig. 2c demonstrates that ξ_{1d} decreases, while ξ_{1s} increases with decreasing k. Both approach 1.0 as k decreases, which agrees with eqn (1) that $D \sim \tau^{-1}$ is exact only when $k \to 0$. Fig. 2d demonstrates that ξ_{2s} approaches 1.0 as $k \to 0$ at low temperatures, but no such trend is observed for ξ_{2d} at high temperatures, and thus the basic presumption $\eta = G_\infty\tau$ in $D \sim T/\tau$ is only a cursory approximation. Although it sometimes gives a consistent result with $D \sim T/\alpha$ for a specific k in a certain temperature range, it depends severely on k and is not fulfilled for all data.

That a is a constant is the presumption of all three SE variants, but some studies have already suggested that it is not a constant.[9,10,13] Below we will show by considering the coordination shell structure that a in water actually varies with temperature, instead of being a constant.

The coordination shell can be statistically depicted as a water molecule drags the effective shells composed of surrounding water molecules to move together. Here we only consider water molecules in the first coordination shell with an effective radius of a, which play the most important role and form a composite along with the central water molecule. The interplay between the central molecule and surrounding water molecules can be described by the coordination number n and the residence correlation time τ_s.[25] The coordination number $n = \int_0^{r_c} 4\pi r^2 g(r)\mathrm{d}r$ is the average number of molecules in the first solvation shell, and r_c = 0.38 nm is the position of the first minimum in the radial distribution function. The residence correlation time τ_s characterizing the lifetime of the first shell is calculated from the residence time correlation function $C(t) = \langle\delta(0)\delta(t)\rangle$ by taking $C(\tau_s) = e^{-1}$, where $\delta(t)$ is 1 if a given molecule is still in the first solvation shell at time t and 0 otherwise.

A larger τ_s corresponds to a larger probability for the molecules to stay in the first shell and move together with the central molecule. The average number of water molecules in the composite is $1 + np(\tau_s)$, where 1 denotes the central molecule and p is the probability of the first shell moving along with the central molecule, which increases monotonically with τ_s. By assuming that both free molecules and the composite are spheres, the effective hydrodynamic radius of the composite is roughly $[1 + np(\tau_s)]^{1/3}a_0$, where a_0 is a constant representing the effective hydrodynamic radius of a free molecule. Because the frictional force applied to the composite $\sim C\eta v[1 + np(\tau_s)]^{1/3}a_0$ should be equal to the sum of the frictional force applied to each molecule in the composite $\sim C\eta v[1 + np(\tau_s)]a$, where v is the velocity of the composite, the average effective hydrodynamic radius can be described by

$$a \sim \frac{a_0}{[1 + np(\tau_s)]^{2/3}} \qquad (2)$$

with τ_s being described by the Arrhenius law $\tau_s = \tau_0 e^{E_a/k_BT}$, where E_a is the activation energy for a molecule to hop out of the first coordination shell and τ_0 is the prefactor, and the probability $p(\tau_s) = \frac{e^{E_a/k_BT}}{(e^{E_a/k_BT} + 1)} = \frac{\tau_s}{\tau_s + \tau_0}$. Eqn (2) then becomes

$$\alpha \sim \frac{\alpha_0}{\left[1 + \frac{n\tau_s}{\tau_s + \tau_0}\right]^{2/3}} \qquad (3)$$

Because τ_0 in eqn (3) is unknown, we still cannot determine the temperature dependence of α. Therefore, we have to first assume that Stokes' formula is established in supercooled water to numerically evaluate $a \sim \alpha/\eta$ and rescale it by its value at T = 390 K for the TIP5P model. The rescaled $\overline{\alpha/\eta}$ plotted in Fig. 3a is approximately constant for T > 280 K but starts to decrease significantly when T < 280 K, which has the same trend as $D \sim (\eta/T)^{-\xi_3}$ shown in Fig. 1c and agrees with previous observations.[8,9,12] We then fit the data in Fig. 3a by eqn (3) with τ_0 being a parameter to be determined. It can be seen that the fitted curve drawn in red in Fig. 3a, which gives τ_0 = 269 ps, almost perfectly matches the numerical data points.

Fig. 3b plots τ_s and n calculated from the simulation data. When the temperature decreases, n decreases because of the more ordered structure of water,[7,26] while τ_s increases because the coupling between molecules becomes stronger. At high temperatures, these two factors contribute oppositely to $np(\tau_s)$ and almost compensate with each other, so the change of a is approximately constant. At low temperatures, the increase of τ_s is much faster than the decrease of n, so $p(\tau_s)$ plays a more significant role than n, leading to a decrease of a. The decrease of $a \sim T/D\eta$ with decreasing temperature has been observed in supercooled water in previous work,[9,10,13] and it also occurs in other liquids, such as supercooled binary Lennard–Jones liquids,[27] supercooled aqueous solutions of glycerol,[28] water/methanol solutions,[29] *ortho*-terphenyl,[30] and tris-naphthylbenzene.[31] Therefore, we conclude that a indeed varies with

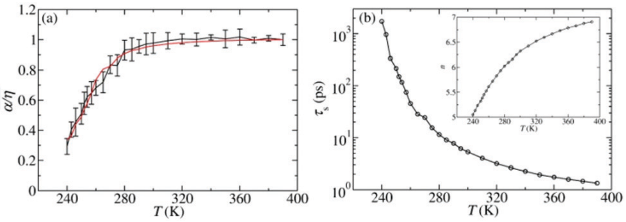

Fig. 3 (a) Rescaled effective hydrodynamic radius $\overline{\alpha/\eta}$ by simulation (black line) and by fitting (red line). (b) Residence correlation time τ_s and coordination number n (inset) *vs.* T.

thermodynamic conditions, which allows the Stokes relation to be valid in supercooled water.

Conclusions

We have performed atomistic MD simulations to explore the validity of the SE relation in supercooled water with the TIP5P model in the range of 240–390 K and the Jagla model in the range of 30–140 K. Consistent with the fact that supercooled water is in its local equilibrium, our results confirm the conservation of the original SE relation in supercooled water, even though its three variants, $D \sim \tau^{-1}$, $D \sim T/\tau$, and $D \sim T/\eta$, all break down and in their fractional forms. The variant $D \sim T/\eta$ gives rational results only when the effective hydrodynamic radius a can be considered as a constant. In addition, because both ξ_1 in $D \sim \tau^{-\xi_1}$ and ξ_2 in $D \sim (\tau/T)^{-\xi_2}$ depend on the wavevector, $D \sim \tau^{-1}$ agrees with $D \sim T/\alpha$ only in the long-wavelength limit, and $D \sim T/\tau$ agrees with $D \sim T/\alpha$ only in a certain temperature range when a specific k is chosen. Although the three variants give similar qualitative results, the exponents are quantitatively different from each other, so τ and τT are not good substitutes of η. Overall, the three variants are usually not good substitutes of the original SE relation, and they should be critically and quantitatively evaluated while they are used to inspect the validity of the SE relation. Besides supercooled water, the inconsistency between the original SE relation and its variants may appear in many other supercooled liquids.

Author contributions

Y. W. conceived and supervised the project. G. R. performed the simulations. Y. W. and G. R. discussed the results and wrote the manuscript.

Conflicts of interest

There are no conflicts to declare.

Acknowledgements

The authors thank Prof. Fanlong Meng for his critical reading of this paper. This work was supported by the Strategic Priority Research Program of Chinese Academy of Sciences (Grant No. XDA17010504), the National Natural Science Foundation of China (No. 11774357, 12047503, and 12104502) and the Science Foundation of Civil Aviation Flight University of China (No. J2021-054 and JG2019-19). The allocation of computer time on the HPC cluster of ITP-CAS is also appreciated.

Notes and references

1 L. D. Landau and E. M. Lifshitz, *Fluid Mechanics*, Pergamon, Oxford, 1987.
2 S. Gupta, J. Stellbrink, E. Zaccarelli, C. N. Likos, M. Camargo, P. Holmqvist, J. Allgaier, L. Willner and D. Richter, *Phys. Rev. Lett.*, 2015, **115**, 128302.
3 D. Bonn and W. K. Kegel, *J. Chem. Phys.*, 2003, **118**, 2005–2009.
4 B. T. Poe, P. F. McMillan, D. C. Rubie, S. Chakraborty, J. Yarger and J. Diefenbacher, *Science*, 1997, **276**, 1245–1248.
5 H. Zhao and H. Zhao, *Phys. Rev. E*, 2021, **103**, L030103.
6 A. Noda, K. Hayamizu and M. Watanabe, *J. Phys. Chem. B*, 2001, **105**, 4603–4610.
7 L. Xu, F. Mallamace, Z. Yan, F. W. Starr, S. V. Buldyrev and H. Eugene Stanley, *Nat. Phys.*, 2009, **5**, 565–569.
8 M. G. Mazza, N. Giovambattista, H. E. Stanley and F. W. Starr, *Phys. Rev. E: Stat., Nonlinear, Soft Matter Phys.*, 2007, **76**, 031203.
9 T. Kawasaki and K. Kim, *Sci. Adv.*, 2017, **3**, e1700399.
10 A. Dehaoui, B. Issenmann and F. Caupin, *Proc. Natl. Acad. Sci. U. S. A.*, 2015, **112**, 12020–12025.
11 S. H. Chen, F. Mallamace, C. Y. Mou, M. Broccio, C. Corsaro, A. Faraone and L. Liu, *Proc. Natl. Acad. Sci. U. S. A.*, 2006, **103**, 12974–12978.
12 I. N. Tsimpanogiannis, S. H. Jamali, I. G. Economou, T. J. H. Vlugt and O. A. Moultos, *Mol. Phys.*, 2019, 1–11, DOI: 10.1080/00268976.2019.1702729.
13 F. Mallamace, C. Branca, C. Corsaro, N. Leone, J. Spooren, H. E. Stanley and S.-H. Chen, *J. Phys. Chem. B*, 2010, **114**, 1870–1878.
14 P. Kumar, S. V. Buldyrev, S. R. Becker, P. H. Poole, F. W. Starr and H. E. Stanley, *Proc. Natl. Acad. Sci. U. S. A.*, 2007, **104**, 9575–9579.
15 E. A. Jagla, *J. Phys.: Condens. Matter*, 1999, **11**, 10251–10258.
16 S. Higuchi, D. Kato, D. Awaji and K. Kim, *J. Chem. Phys.*, 2018, **148**, 094507.
17 H. J. C. Berendsen, D. van der Spoel and R. van Drunen, *Comput. Phys. Commun.*, 1995, **91**, 43–56.
18 D. Van Der Spoel, E. Lindahl, B. Hess, G. Groenhof, A. E. Mark and H. J. Berendsen, *J. Comput. Chem.*, 2005, **26**, 1701–1718.
19 S. Nosé, *J. Chem. Phys.*, 1984, **81**, 511–519.
20 W. G. Hoover, *Phys. Rev. A: At., Mol., Opt. Phys.*, 1985, **31**, 1695–1697.
21 U. Essmann, L. Perera, M. L. Berkowitz, T. Darden, H. Lee and L. G. Pedersen, *J. Chem. Phys.*, 1995, **103**, 8577–8593.
22 B. Hess, *J. Chem. Phys.*, 2002, **116**, 209–217.
23 B. J. Alder and T. E. Wainwright, *Phys. Rev. Lett.*, 1967, **18**, 988–990.
24 J. P. Boon and S. Yip, *Molecular hydrodynamics*, Courier Corporation, 1991.
25 S. Koneshan, J. C. Rasaiah, R. Lynden-Bell and S. Lee, *J. Phys. Chem. B*, 1998, **102**, 4193–4204.
26 R. Shi, J. Russo and H. Tanaka, *Proc. Natl. Acad. Sci. U. S. A.*, 2018, **115**, 9444–9449.
27 F. Affouard, M. Descamps, L.-C. Valdes, J. Habasaki, P. Bordat and K. L. Ngai, *J. Chem. Phys.*, 2009, **131**, 104510.
28 B. Chen, E. E. Sigmund and W. P. Halperin, *Phys. Rev. Lett.*, 2006, **96**, 145502.
29 C. Corsaro, E. Fazio and D. Mallamace, *J. Chem. Phys.*, 2019, **150**, 234506.
30 Z. Shi, P. G. Debenedetti and F. H. Stillinger, *J. Chem. Phys.*, 2013, **138**, 12A526.
31 S. F. Swallen, P. A. Bonvallet, R. J. McMahon and M. D. Ediger, *Phys. Rev. Lett.*, 2003, **90**, 015901.